Seismic monitoring of the Northparkes lift 2 block cave—part I undercutting

by M. Hudyma*, Y. Potvin†, and D. Allison§

Synopsis

Caving of the second lift of the E26 orebody at Northparkes Mines was monitored with a comprehensive package of instrumentation, including an ISS seismic monitoring system. Seismicity was collected by an array of 19 triaxial accelerometers and 9 uniaxial geophones, giving a high quality seismic data set. The seismic response to block caving at Northparkes has been divided into two papers. The first paper focuses on the seismicity during undercutting. The second paper deals primarily with the seismicity during cave propagation during initial cave production.

In this paper, traditional seismic monitoring concepts are applied to seismicity during cave mining. More than 40 000 seismic events were recorded during cave undercutting between February and January 2004. Events up to local magnitude +1.3 were recorded near the mine during undercutting, with event rates of up to 500 per day. Analysis of frequency-magnitude distributions, S-wave to P-wave energy, and temporal variations in event magnitude all gave insight into the seismicity recorded. In addition, a new technique, called apparent stress time history, was shown to be sensitive to stress change from undercut blasting, and useful to identify significant periods during cave development.

A significant difference was identified between the cave back location and the halo of seismic events above the cave. Throughout the undercutting, the aseismic zone of loosening was typically 50 to 70 metres in vertical thickness. Based on the seismicity, a stress driven rock mass failure model is proposed. Early in the undercutting, seismicity and movements in the seismogenic zone were directly triggered by stress change from undercutting. Towards the end of undercutting, seismicity was virtually uncorrelated with undercut blasting, and likely due to the onset of cave initiation.

Introduction

Northparkes Mines is a block caving operation located near Parkes, New South Wales, Australia. Lift 2 of the mine is extracting a 24 million ton copper, gold reserve in the lower E26 orebody, containing 0.47 g/t gold and 1.21% copper[1]. The base of the Lift 2 mining block sits approximately 900 m beneath surface and extends up 350 m nearly directly underneath the mined-out Lift 1 block. The footprint is approximately 180 m in the north-south direction and 160 m east-west.

Geology and geotechnical setting

There are four major rock types that are intersected by the Lift 2 cave at Northparkes (Figure 1).

- *Quartz monzonite porphyry*—the orebody is composed of a stockwork of subvertical quartz fingers and veins and disseminations
- *Volcanics*—located to the west of the orebody, the volcanics unit is a Late Ordovician trachyandesite[2]
- *Biotite quartz monzonite*—a volcanic unit located on the east of the orebody
- *Diorite*—an intrusion of diorite intersects the orebody between Lift 1 and Lift 2 from the west side of the orebody. The diorite unit is slightly weaker than the volcanics rock types.

Typical intact rock strengths are presented in Table I.

In situ stress measurements using CSIRO HI cells were taken at a depth of 813 metres. The results of the measurements (shown in Table II) indicate a sub-horizontal east-west maximum principal stress.

Mining

Key periods of seismic and mining activities associated with extraction of Lift 2 at Northparkes Mines are shown in Table III.

The time and location of each of the 290 Lift 2 undercut blasts (Figure 2) is documented in an RMIT undergraduate thesis[6]. The undercut blasting information allows detailed cause-effect analysis of the extraction of the undercut versus the mining-induced seismicity.

* *Itasca Consulting Canada Inc.*

† *Australian Centre for Geomechanics.*

§ *Rio Tinto.*

Seismic monitoring of the Northparkes lift 2 block cave—part I undercutting

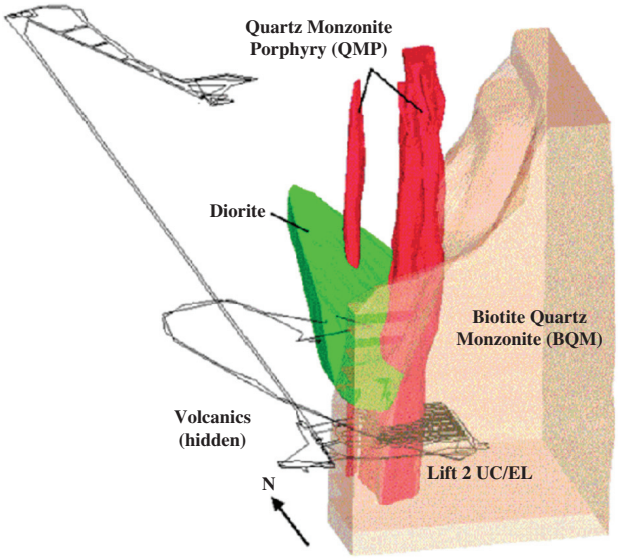

Figure 1—Geological units near the Lift 2 orebody at Northparkes Mines[3]

Table I

Intact rock strengths in the E26 orebody at Northparkes[4]

Rock type	Number of samples	Uniaxial compressive strength (MPa)
Volcanics	66	116
Quartz monzonite porphyry	44	124
Biotite quartz monzonite	35	143

Table II

Pre-mining *in situ* stress at Northparkes[5]

Depth (m)	Principal stresses	Magnitude (MPa)	Dip (deg.)	Bearing (deg.)
~813 m	σ1 σ2 σ3	53.2 33.1 22.2	10 01 80	096 186 283

Table III

Seismic monitoring and mining activities in Lift 2

Time period	Mining activity
1 Sept 2002	Start of seismic record for Lift 2 Development mining in the crusher and undercut
25 Feb 2003–21 Jan 2004	Undercut blasting and crusher development
21 Jan 2004–21 Aug 2004	Development of production level
21 Aug 2004–Dec 2004	Initial cave production and propagation

Seismic monitoring in caving mines

The use of cave mining techniques is steadily increasing in Australia. There are several sublevel and block caving mines currently in operation in Australia, with several more in the development and feasibility stages. The failure mechanisms involved in the rock mass during the caving processes are not well understood and are inherently difficult to monitor with visual observations and conventional instrumentation, such

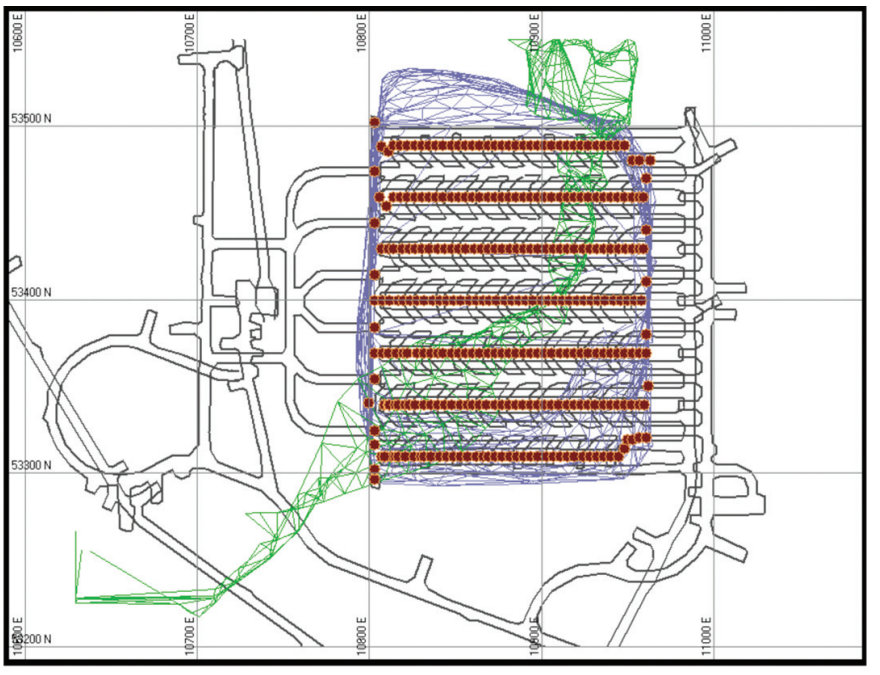

Figure 2—Location of the undercut blasts for Lift 2[6]. The cave profile is shown with the blue wireframe around the blasts, whereas a major contact between the BQM and volcanics units is shown with a green wireframe that crosses the mining from the south-west to the north-east

as extensometers and stress cells. While cave mining has been used for decades, it is only in the last decade that seismic monitoring systems have been installed to monitor caving-related rock mass failure. There are only a handful of mines in the world in which good quality seismic data associated with the caving process have been collected.

Based on seismic data from Lift 1 of the Northparkes block cave, Duplancic[7] proposed a conceptual caving model involving a number of zones identified by the condition of the rock mass (Figure 3). The zones are:

- *Cave zone*—composed of rock blocks of caved material
- *Air gap*—in continuous caving, the height of the air gap is a function of production draw rate
- *Zone of loosening*—large-scale displacements of the rock mass are occurring. Loss of confinement in the rock mass controls failure in this area. There is no seismicity in this area
- *Seismogenic zone*—active seismic front caused by failure of the rock mass, primarily through shearing and intact rock fracturing
- *Pseudo-continuous domain*—elastic deformation is occurring in the rock mass above the seismogenic zone.

Butcher[8] notes an important distinction in cave behaviour. Cave initiation occurs during and directly following undercutting, and is characterized by relatively low rates of caving, typically less the 0.5 to 1 metre per day. Cave propagation is a brief phase of accelerated rock mass deformation that typically occurs following cave initiation. The rate of caving during cave propagation is typically a few to several metres per day. Butcher[8] also notes that concurrent with cave propagation, there is a general destressing of the area near the cave, with stress shed to abutment areas, potentially up to a few hundred metres away.

Seismic monitoring for Lift 2 at Northparkes

The Northparkes seismic system is composed of an array of 19 triaxial accelerometers and 9 uniaxial geophones sites, giving a high quality seismic data set[9]. An orthogonal view of the seismic sensors is shown in Figure 4. The sensors are concentrated close to the cave to provide high sensitivity.

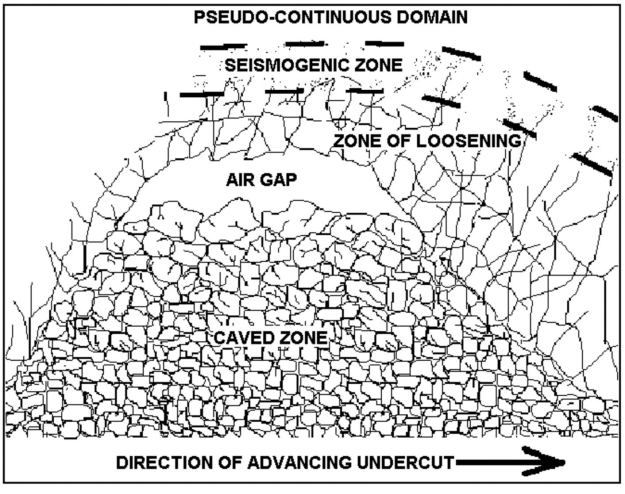

Figure 3—Zones of ground behaviour in a block caving mine[7]

The sensors are configured in a three dimensional array around the orebody to ensure accurate locations and to minimize the effects of sensor blinding on event locations and seismic system sensitivity as the cave progresses.

Seismic monitoring of the Lift 2 cave at Northparkes Mines began in September 2002. More than 60 000 seismic events detected between September 2002 and January 2006, during undercutting and the first few months of production caving. Events up to local magnitude +2.9 were recorded near the mine during caving, with event rates of up to 500 per day. Operation of the seismic system was well managed with no significant system interruptions or data loss, resulting in a good seismic record for the Lift 2 cave.

Mine seismology applied to Northparkes Lift 2

A number of mine seismology data analysis techniques and concepts have been applied to compare and contrast general trends in seismicity during undercutting and cave production.

Frequency-magnitude analysis

Frequency-magnitude analysis of seismic events was first proposed in earthquake seismology[10]. It was recognized that the relation between the frequency of occurrence and the magnitude of seismic events follows a power law. When data are plotted on a frequency of occurrence versus magnitude chart, the absolute value of the slope of the line is referred to as the b-value. The b-value for large populations of seismic events is typically close to 1.0. While this relation holds true for large subsets of data, when one analyses individual groups of seismic events, the b-value may vary quite dramatically, depending upon the mechanism of the seismicity. Fault-slip related seismicity frequently has a very low b-value (often less than 0.8). Seismicity associated directly with stress change due to mine blasting frequently has a b-value in the range of 1.2 to 1.5[11]. Frequency-magnitude analysis of seismic events is one of the most widely used techniques for seismic hazard analysis.

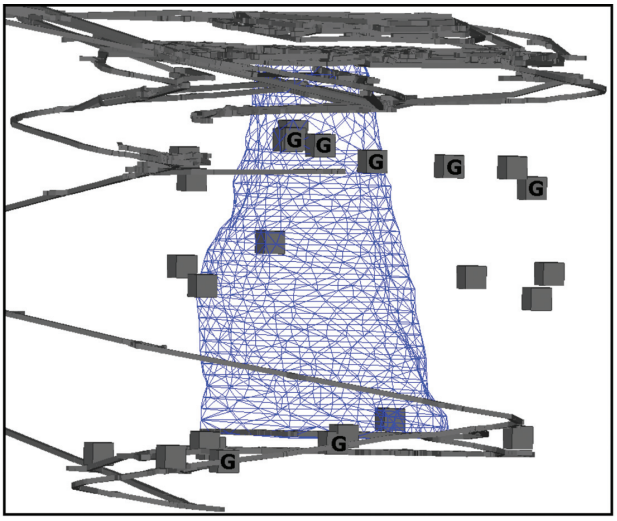

Figure 4—Location of seismic sensors around the Lift 2 cave at Northparkes. Uniaxial geophones are identified with a 'G'. The final cave profile is shown with a wireframe

A frequency-magnitude relation for the seismicity recorded at Lift 2 is shown in Figure 5.

The frequency-magnitude relation in Figure 5 shows that the Northparkes seismic data has a bimodal frequency-magnitude relation, suggesting that the mechanisms of smaller events may not be related to the mechanisms of very large events in the mine. A bi-modal relation is not unexpected for a large dataset. Numerous authors have reported bimodal and multimodal frequency-magnitude relations for large datasets, largely due to multiple source mechanisms of mine seismicity[12,13,14]. Almost all of the local magnitude +1 events occurred in a two-month time period during the connection of the Lift 2 and Lift 1 caves in late 2004.

Figure 5 also shows the minewide sensitivity of the seismic system is approximately local magnitude –1.9. This is a 'data-processing driven' sensitivity, as there are virtually no events in the seismic record with a local magnitude less than –2, i.e. events smaller than local magnitude –2 were rejected from the database.

There are significant differences in the seismic response to mining for different lithological regions around the mine. Figure 6 shows the locations of the significant events at Northparkes (local magnitude ≥ 0). There are few significant events and almost no large events (local magnitude ≥ +1) on the south-east side of the orebody in the BQM rock type. Figure 7 shows the locations of the smaller events at Northparkes (local magnitude < 0). The smaller events are more evenly spatially distributed around the orebody, although many of the events in the BQM unit are located close to the BQM-volcanics and BQM-diorite contacts.

Temporal variations in event magnitude

Magnitude-time history analysis (plotting of event magnitude changes over time) can be particularly insightful in understanding the seismic response to mining, giving indications of both seismic hazard and seismic source mechanism. In a magnitude-time history chart, each seismic event is plotted chronologically, and the cumulative number of events is shown as an incremental line corresponding to the secondary y-axis. A magnitude-time history chart for the events during undercutting and initial caving at Lift 2 is shown in Figure 8. The slope of the 'cumulative number of events' line is the seismic event rate. Changes in slope indicate how the seismic event rate changes over time.

Magnitude-time history charts provide several valuable pieces of information about a population of seismic events.

- The cumulative number of events indicates the processes that are driving the rock mass failure. 'Step-wise' behaviour of the cumulative number of events is an indication of a strong rock mass response to blasting. The frequency of occurrence of seismic events is high for a short period after the blast, but decreases typically in a few hours. During the early stages of Lift 2 undercutting, seismicity was strongly controlled by blasting (Figure 9)
- A constant slope of the 'cumulative number of events' trend is an indication that seismicity is not triggered directly by mine blasting, which is commonly the case for fault-slip or structurally related seismicity. Changes in slope indicate a change in the rate of the rock mass

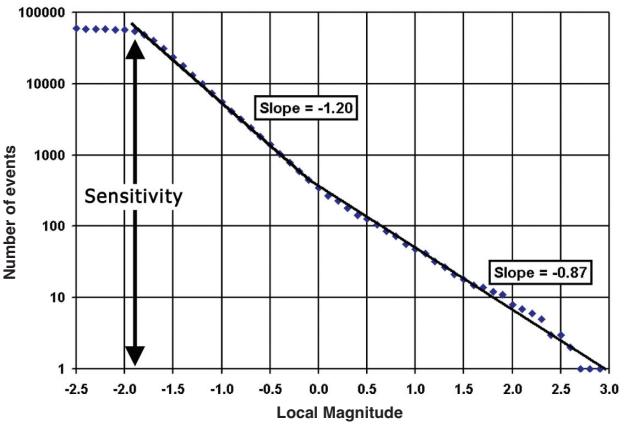

Figure 5—Frequency-magnitude relation for seismic events associated with the Lift 2 block cave

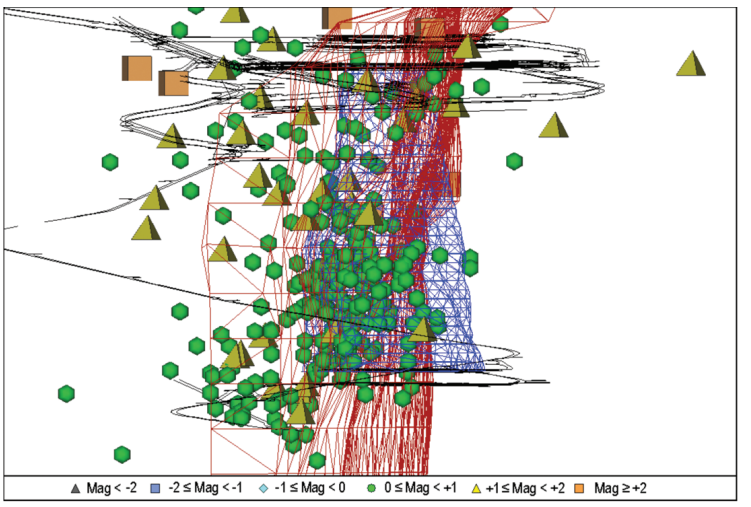

Figure 6—Locations of the significant events at Northparkes (local magnitude ≥ 0). The BQM contact is shown in red, with BQM on the right (south-east) and volcanics on the left (north-west)

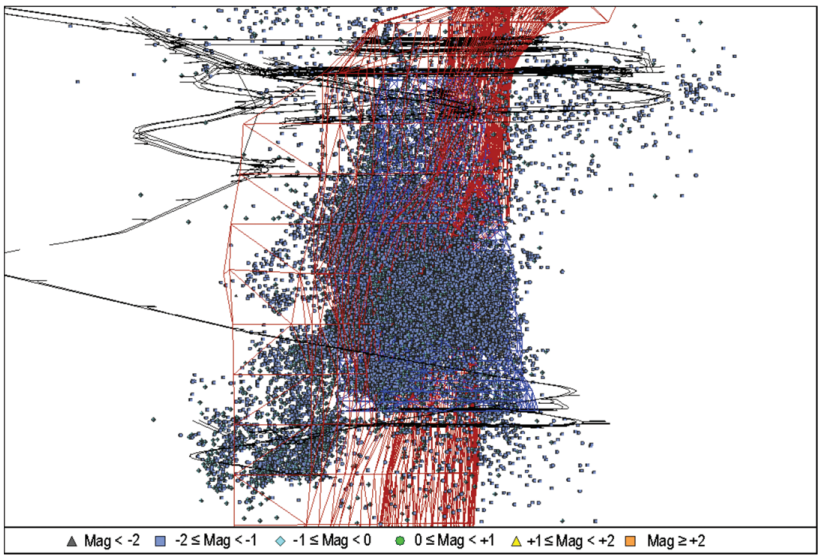

Figure 7—Locations of the smaller events at Northparkes (local magnitude < 0)

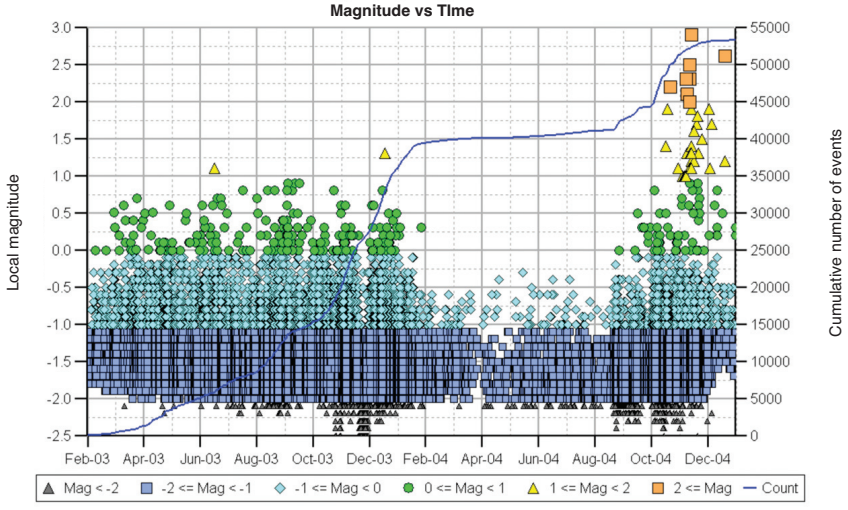

Figure 8—Magnitude-time history chart for the seismic events during undercutting and initial caving at Northparkes Lift 2

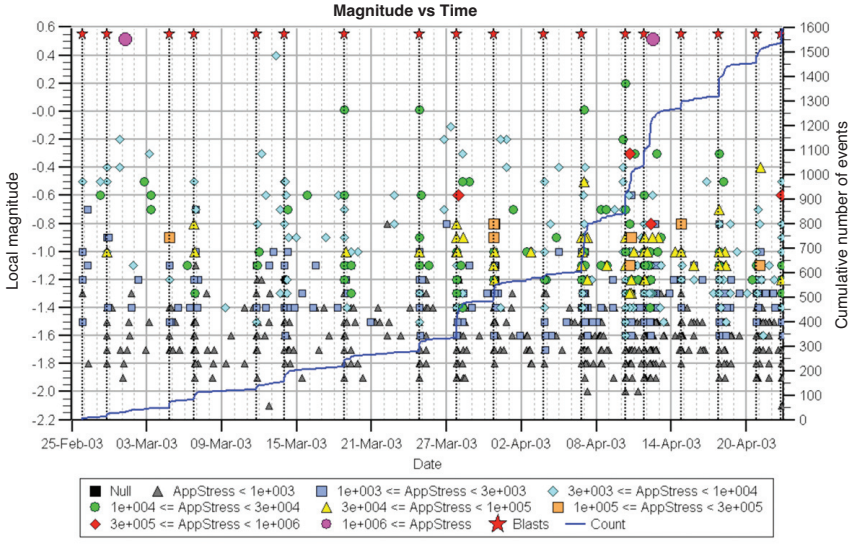

Figure 9—Magnitude-time history chart for the first 2 months of undercutting at Lift 2. The 'step-wise' shape of the cumulative number of events line is typical of stress driven seismicity. The star symbols and vertical dotted lines indicate the occurrence of undercut blasts

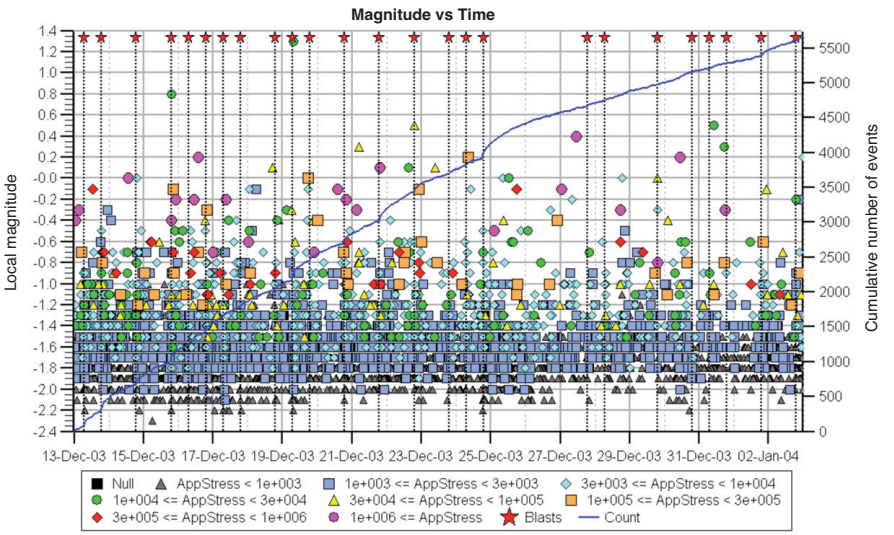

Figure 10—Magnitude-time history chart for seismic events for blasts near the end of undercut blasting. The star symbols and vertical dotted lines indicate the occurrence of undercut blasts

failure process. During the later stages of (September 2003 to January 2004) undercutting Lift 2, the relationship between seismicity and undercut blasting became weaker, resulting in a constant rate of seismic events (Figure 10). There are few significant increases in event frequency after undercut blasts, and the rate of seismic events is relatively constant, even during periods of no blasting (24–27 December, 2003)

- The timing of the largest events in the population shows changes in seismic hazard. If the largest event increases over time, the dimensions of the rock mass failure at the seismic source may be increasing in size, and seismic hazard may be increasing
- The occurrence of the largest events compared to changes in seismic event rate indicates whether mine blasting is directly triggering the larger events. For structurally controlled seismicity, the largest events do not occur at the same time as the majority of events (as shown by steps or changes in slope in the 'cumulative number of events' line)
- Essentially, a magnitude-time history chart gives a chronology of the rock mass failure process, giving indications of seismic source mechanism and seismic hazard.

S-wave to P-wave energy ratio analysis

Past research has found that the ratio of S-wave to P-wave (S:P) energy for a seismic event is a good indicator of seismic source mechanism[15]. Events with a high S:P energy ratio (S:P>10) are typically associated with shearing along existing geological features[16,17]. Events with a low S:P energy ratio (S:P<3) are more commonly related to stress fracturing or volumetric fracturing failure mechanisms[18]. Duplancic[7] found that shear-related events during caving of Lift 1 at Northparkes had high ratios of S-wave to P-wave energy. Events with an S:P energy ratio near one have been found to be associated with tensile seismic source mechanisms[19].

Figure 11 is a scatterplot comparing S-wave to P-wave energy, showing a scale dependence (particularly for events smaller than local magnitude –1). Smaller events tend to have a lower S:P wave energy, suggesting a scale dependence of seismic source mechanism.

Figure 12 is an S:P energy cumulative distribution for different magnitude ranges for the Northparkes data. Overall, the seismic source mechanism is shear, with 60–80% of all events having an S:P energy ratio greater than 10. The percentage of 'non-shear' events with low S:P energy ratios (S:P < 3) is less than 10%. However, for the smallest events (local magnitude < -2.0), only 40% of the events have an S:P energy ratio greater than 10, compared to 64% or more for all of the other magnitude ranges. For the larger magnitude ranges ($M_L \geq -1$), the percentage of events with an S:P energy ratio greater than 10 is relatively consistent, between 64% and 78%.

In summary, the very small events are more non-shear than the events larger than –2. The local magnitude –1 and larger events are very similar.

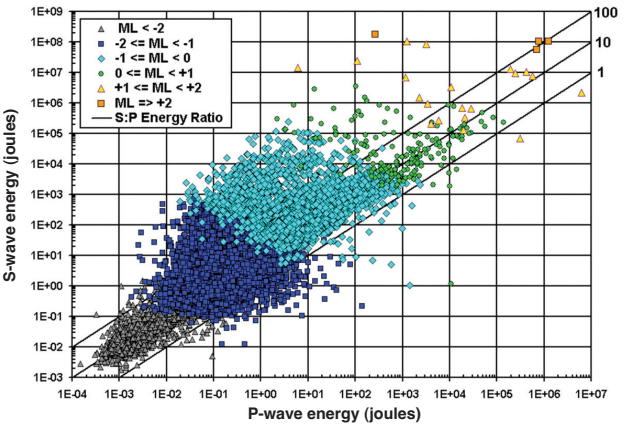

Figure 11—S-wave energy to P-wave energy scatter plot. The lines refer to S:P energy ratios of 1, 10 and 100. There appears to be a scale dependence of S:P energy ratio for smaller events, although it is hard to quantify from this scatter plot

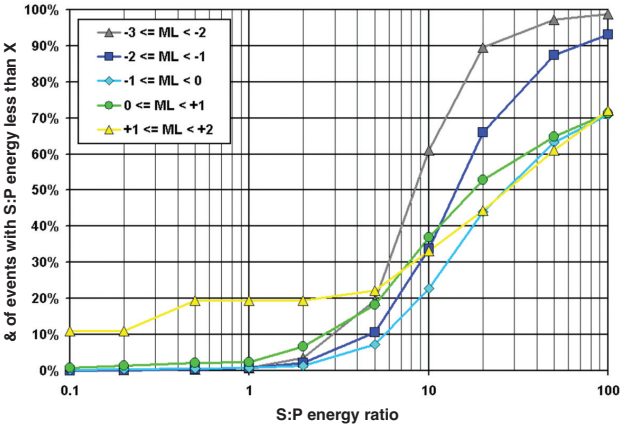

Figure 12—S:P energy ratio for various magnitude ranges at Northparkes. There is a scale dependence of S:P energy ratio for events smaller than local magnitude –1 and particularly for events smaller than local magnitude –2

Apparent stress time history

Past work has shown that seismic events associated with increasing stress typically have a higher than expected seismic energy release[20,21]. Instability analysis utilizes this concept to identify regions of increasing and decreasing stress in an effort to identify unstable rock mass conditions that are potentially prone to large damaging seismic events[22].

Background

Apparent stress is a model independent measure of the stress change associated with an event[23]. Originally proposed by Wyss and Brune[24], apparent stress is defined as:

$$\sigma_a = \mu E / Mo \qquad [1]$$

where

σ_a = apparent stress

μ = the shear modulus of rigidity of the source material,

E = seismic energy, and

Mo = seismic moment.

Apparent stress is a scale dependent seismic source parameter, increasing with event size[23].

From a practical application perspective, higher stress regions of a mine tend to release more seismic energy and tend to have relatively lower amounts of deformation due to higher confining stress, resulting in higher apparent stress seismic events[21]. Similarly, apparent stress was used to identify areas of high stress associated with block caving related seismicity at Palabora[25]. It was also observed that lower apparent stress events were often found in lower stress areas, or areas that have shed load due to general rock mass fracturing and failure[21].

A mine seismicity parameter called energy index can be useful to identify regions of increasing and decreasing stress in an effort to identify unstable rock mass conditions that are potentially prone to large damaging seismic events[22]. Energy index is the ratio of the amount of energy recorded compared to the expected energy for an event of a particular size. Chen[26] found that seismic events in the seismogenic zone near the apex of the cave tended to have a higher energy index.

Figure 13 shows a energy-moment relation for 19280 events recorded over a period of 3 years in an Australian mine[27]. Figure 14 (left) shows the events that have a high Energy Index (in this case a 'high' Energy Index identified if the actual energy recorded is 5 times greater than the expected energy). Figure 14 (right) shows the events that have a high Apparent Stress (in this case high Apparent Stress is arbitrarily chosen to be greater than 50,000 Pascals).

It is observed from the two plots that of the 19 280 events, 2428 events have high Apparent Stress and high energy index. So to a degree the two methods of identifying higher energy events are similar. However, 71% of the high energy index events have a local magnitude less than -1, while only 4% of the high energy index events have a local magnitude greater than 0. For apparent stress, 40% of the high apparent stress events have a magnitude of less than –1, while 15% of the high apparent stress events have a local magnitude greater than 0. Effectively, trends in energy index are more related to stress associated with smaller events, while trends in high apparent stress are more related to stress associated with larger events.

Apparent stress time history

Apparent stress time history (ASTH) is proposed as a technique to identify time periods in which there is a high frequency of occurrence of events with a high apparent stress, potentially due to high stress conditions. A minimum apparent stress threshold is chosen, ideally identifying events that have anomalously high apparent stress. A threshold value of 10 000 to 30 000 Pascals is often a good threshold (usually the top 10 to 20 percentile of high apparent stress events). The apparent stress frequency is the daily average of high apparent stress events over a trailing time period of several hours to a few days. If the averaging time period is too short, the daily apparent stress frequency is very sensitive and fluctuates excessively. If the averaging time period is too long, the daily apparent stress frequency will display general trends, but may be too insensitive to clearly identify changing stress conditions.

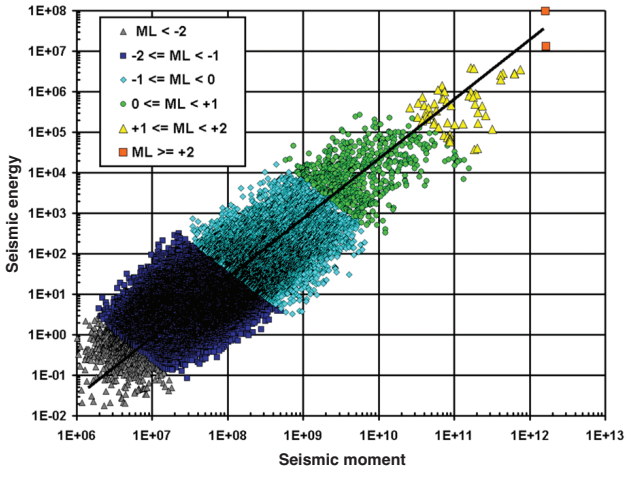

Figure 13—Energy-moment relation for 19 280 events recorded over a period of 3 years in an Australian mine

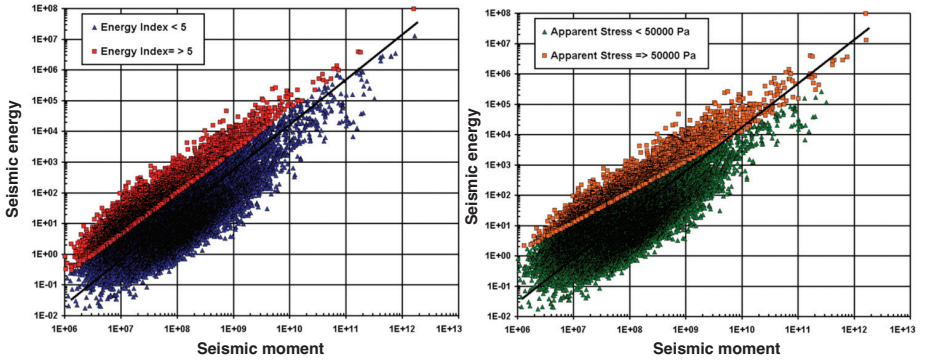

Figure 14—The left diagram shows the events with a high energy index (EI ≥ 5; square red points). The right diagram shows the events with a high apparent stress (apparent stress ≥ 50 000 Pascals; square orange points)

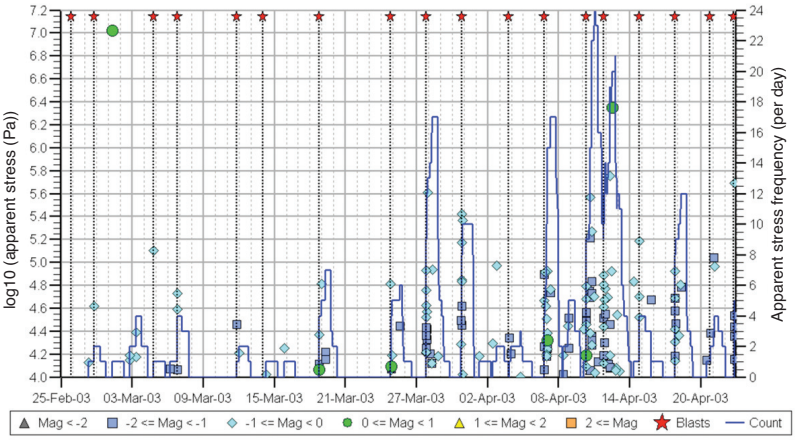

Figure 15—ASTH chart for the first two months of undercutting

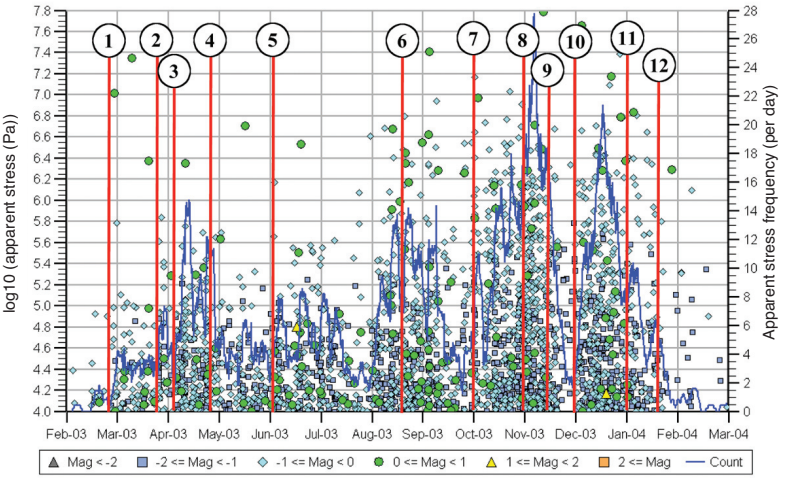

Figure 16—Apparent stress time history for undercutting at Northparkes Lift 2, from February 2003 to January 2004

In an ASTH chart, the apparent stress of each of the events in the population is plotted by apparent stress, time and another parameter such as event magnitude. Plotting the parameters of individual events helps the user to see trends in data. For example, an ASTH chart for the first two months of undercutting is shown in Figure 15. The times of the first[18] undercut blasts are also identified in Figure 15. Each blast results in an increase in apparent stress in the events recorded. In most cases, the increase in apparent stress in the events occurs for only a few hours after an undercut blast. Figure 15 shows that as the size of the undercut increases, there is progressively higher apparent stress in the induced seismicity.

Increases in apparent stress have been found to be strongly related to stress change due to mine blasting[27]. In some cases, a high level of apparent stress frequency may be a good indicator of elevated seismic hazard, particularly in high stress mining environments.

Apparent stress time history at Northparkes

An ASTH is shown for the undercutting of Lift 2 in Figure 16

and for the initial few months of production caving in Figure 17. Key periods in the seismic record are denoted in Figure 16 and Figure 17, and are listed in Table IV.

Undercutting Lift 2

Based on the observations in the seismicity, undercutting has been separated into three distinct phases (Figure 18):

- Early undercutting—February–April 2003,
- Middle undercutting—late April–August 2003, and
- Late undercutting—September 2003–January 2004.

The number of seismic events is compared to the number of undercut blasts in Figure 19. The seismic event rate increases in the early undercutting and is relatively constant in the middle undercutting phase (until late August 2003). By the late undercutting phase, the seismic event rate has increased substantially.

Early undercutting—February–April 2003

The seismicity during the early undercutting phase shows that events occur directly above undercut blasts, with the elevation of the events gradually increasing in elevation to up to 30 metres above the blasts (Figure 20). Most events occur directly after undercut blasts, with relatively few events between blasts. More than 40% of the events occurred within 1 hour of the undercut blast, and more than 80% of events occurred within 4 hours of the undercut blast. Figure 9 is a magnitude-time history chart for the early undercutting phase showing intense seismicity directly after blasts.

The high apparent stress events occur directly after mine blasts (Figure 9), when stress change would be occurring. Figure 15 shows an ASTH chart for this time period. For the first several blasts, there are few high apparent stress events, but as blasting progresses, the number of high apparent stress events increases significantly.

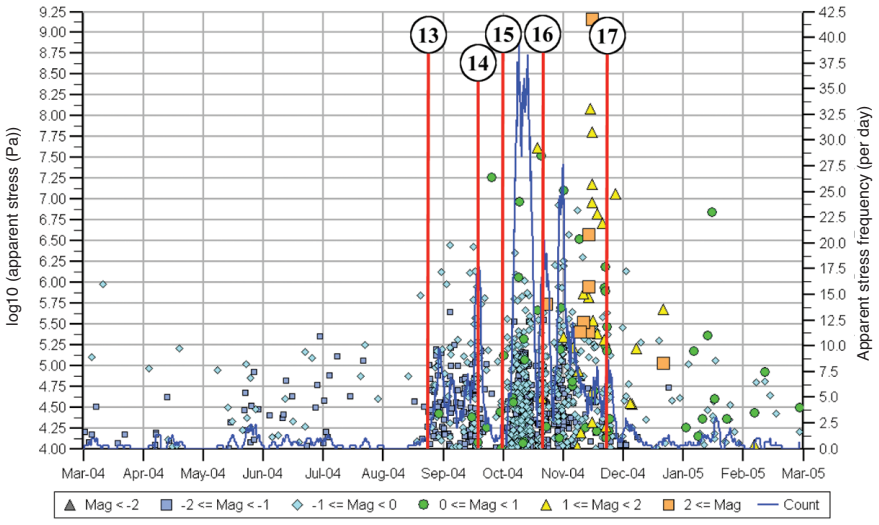

Figure 17—Apparent stress time history for the initial caving period at Northparkes Lift 2, from August 2004 to December 2004

Table IV

Significant periods in the seismic record at Northparkes Lift 2

1.	25 Feb 2003—start of undercutting.
2.	Late March 2003—second set of undercut rings is started.
3.	03 April 2003—undercutting widens to the third set of rings to the north.
4.	26 April 2003—seismicity runs up the BQM contact after blast 26 April.
5.	03 June—fourth set of undercut rings is started.
6.	16 August 2003—microseismic event rate triples from 35 events per day to 100 events per day—undercutting widens to the fifth set of rings to the north—seismogenic zone steps out to the north-east.
7.	October 2003—undercutting rate goes from 2 000 m^2 in September 2002 to 9 000 m^2 in October 2003.
8.	November 2003—north end of undercut widens by 50% from 50 metres to 75 metres.
9.	20 November 2003 @ 19h00—calibration of seismic system appears to have been adjusted. There is a clear order of magnitude decrease in energy and moment seismic source parameters.
10.	30 November 2003—calibration of system is changed back to previous settings.
11.	January 2004—undercutting rate decreases from 7 000 m^2 in December 2003 to 3 000 m^2 in January 2004.
12.	21 January 2004—undercut blasting is complete.
13.	21 August 2004—production cave draw starts.
14.	16 September 2004—cave production halted for 14 days.
15.	30 September 2004—cave production restarted.
16.	19 October 2004—local magnitude +2 event. First of the several very large seismic events associated with connection between the Lift 2 and Lift 1 caves.
17.	23 November 2004—microseismic event rate drops from 60 events per day to 15 events per day. Visual observations found that the crown pillar had failed at this stage. however, physical displacement connection between the caves is believed to have occurred in early 2005.

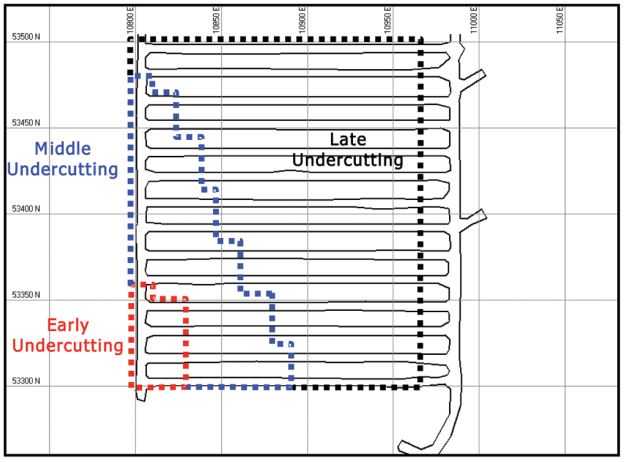

Figure 18—Plan view schematic of the three stages of undercutting

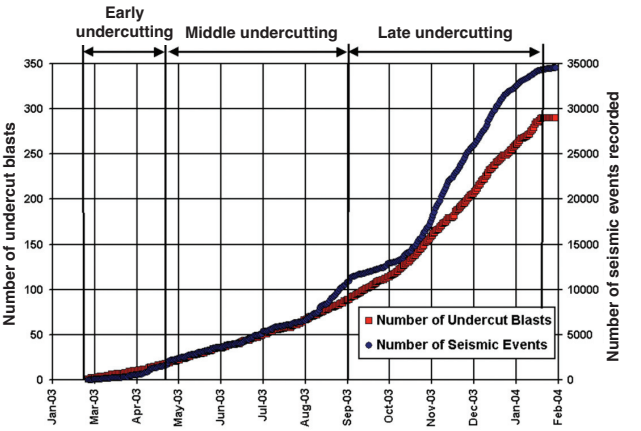

Figure 19—Number of undercut blasts versus the number of seismic events recorded

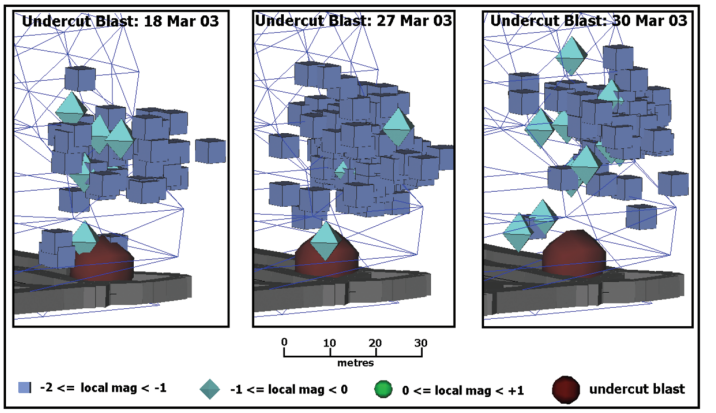

Figure 20—Seismic events following three undercut blasts during the first phase of undercutting

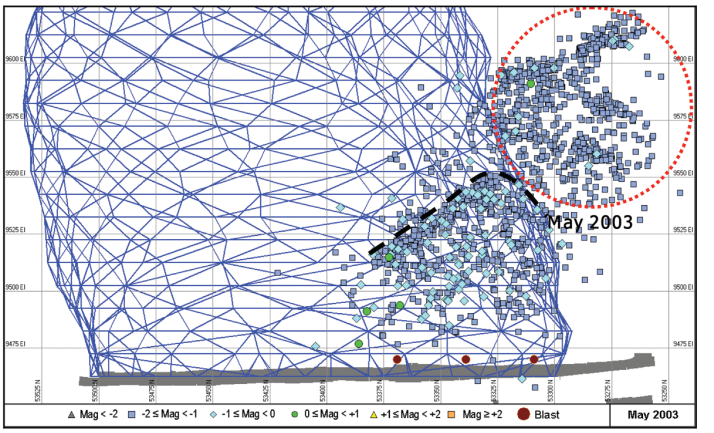

Figure 21—Events during May 2003. The top of the 'seismogenic zone' at the end of the month is denoted by a dashed line

The seismicity in the first phase of undercutting suggests that the rock mass deformation is being induced by the undercut geometry changes, with limited or no rock mass deformation (caving) occurring between blasts. The recorded seismicity follows an expected trend of a seismogenic zone developing over the undercut and gradually increasing in elevation.

Middle undercutting—April–August 2003

During the second phase of undercutting, seismicity was less predictable than in the first phase. Geological features started to play a significant role in the seismicity. There was a rapid progression of events upwards along the diorite/BQM contact, to an elevation more than 80 metres above the expected cave back. There were also significant levels of seismicity on the diorite/BQM contact to the south of the cave footprint (red circled area in Figure 21).

Movements in the seismogenic zone were inconsistent, moving significantly in some months (25 to 40 metres in elevation in June 2003) and hardly moving at all in other

months (Figure 21 to Figure 24). There was a lack of seismicity on the north and east sides of the cave, making identification of the full seismogenic zone difficult.

The number of events and timing of events was relatively consistent in May and June 2003. However, by August 2003, the event rate had almost tripled, and most seismic events were no longer directly triggered by undercut blasts. This suggests that the seismicity was starting to be caused by a more continuous rock mass failure process, rather than being induced by each discrete undercut blast.

Late undercutting—September 2003–January 2004

The locations of the seismic events due to undercutting from September 2003 to January 2004 are shown monthly in a series of isometric views in Figure 25. The figures also show the progression of the undercut blasting over the 5 months. From September 2003 to January 2004, approximately 75% of the undercut was extracted, and almost 28 000 seismic events were recorded. The eastern bound of the seismogenic zone is shown for each month in Figure 25. The seismogenic

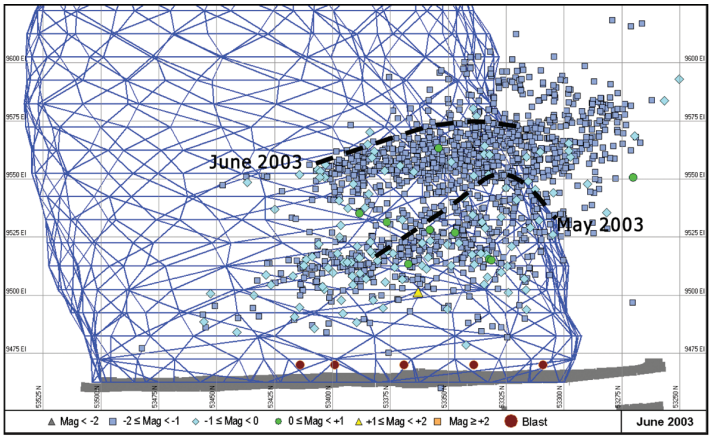

Figure 22—Events during June 2003. The top of the 'seismogenic zone' at the end of the month is denoted by a dashed line

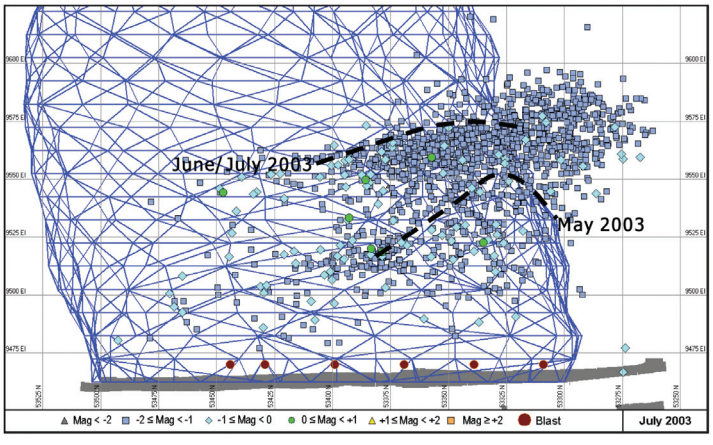

Figure 23—Events during July 2003. The top of the 'seismogenic zone' at the end of the month is denoted by a dashed line

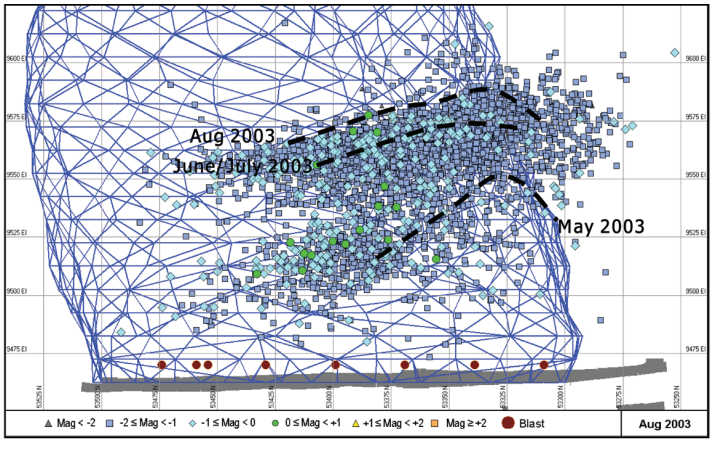

Figure 24—Events during August 2003. The top of the 'seismogenic zone' at the end of the month is denoted by a dashed line

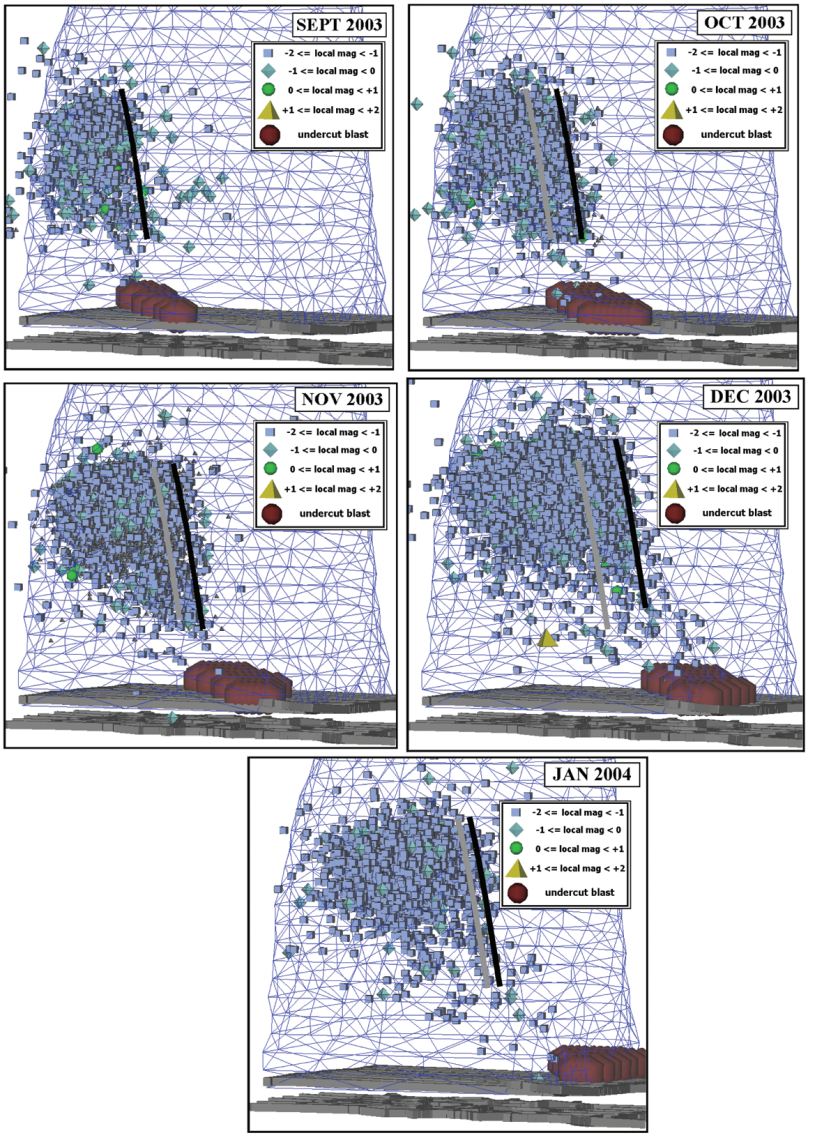

Figure 25—Isometric views of the seismicity during the late undercutting stage at Lift 2. The dark line in each view shows the approximate limit of the seismicity. The gray line shows the seismic limit of the previous month. The month-by-month extraction of the undercut is also shown on each diagram

zone is approximately 25 to 50 metres in vertical height and increases in elevation by only about 25 metres during this period.

The seismogenic zone does move horizontally somewhat towards the north-east, as the undercut moves to the north-east. However, there is surprisingly little seismicity near the undercut blasting. The seismicity tends to continue to occur in the peak of the cave. Frequency-magnitude analysis showed the lack of events was not due to a reduction in the seismic system sensitivity. The lack of seismicity was likely due to the fact that the undercut has been extended fully to the north, with all the remaining undercut blasts are in a stress shadow of the east-west maximum principal stress.

As the undercut mining progresses, the seismicity tends to concentrate in the south side of the cave, with almost no seismicity in the northern 50 metres of the cave. This aseismic band is shown in the January 2004 seismicity picture in Figure 26. This is particularly surprising since all of the undercut blasts in January 2004 were on the north side of the undercut. There is no clear geological reason for the aseismic zone as the three primary rock units (Lower Volcanics, Diorite, and BQM) are all present in the north side of the orebody.

Apparent stress in the seismogenic zone

Throughout undercutting of Lift 2, the seismogenic zone was large and diffuse. Clear movements in the seismogenic zone were often difficult to identify. The locations of high Apparent stress events were used to identify movements in the seismogenic zone. The assumption is that the high Apparent stress events are most likely to occur in the area of highest stress change, which would be the apex of the seismic failure front. Figure 27 shows the location of the high Apparent Stress events (Apparent Stress ≥ 10,000 Pascals) on a month-by-month basis for July, August and September 2003. A red-line is interpreted at the bottom of each month's seismicity (red-lines from previous months are coloured black

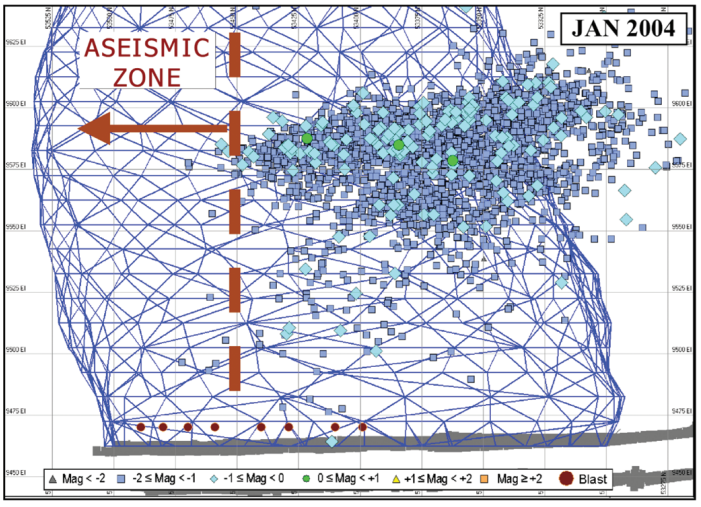

Figure 26—Location of the seismic events in January 2004 (looking east). There is an aseismic region of the cave on the north side of the orebody

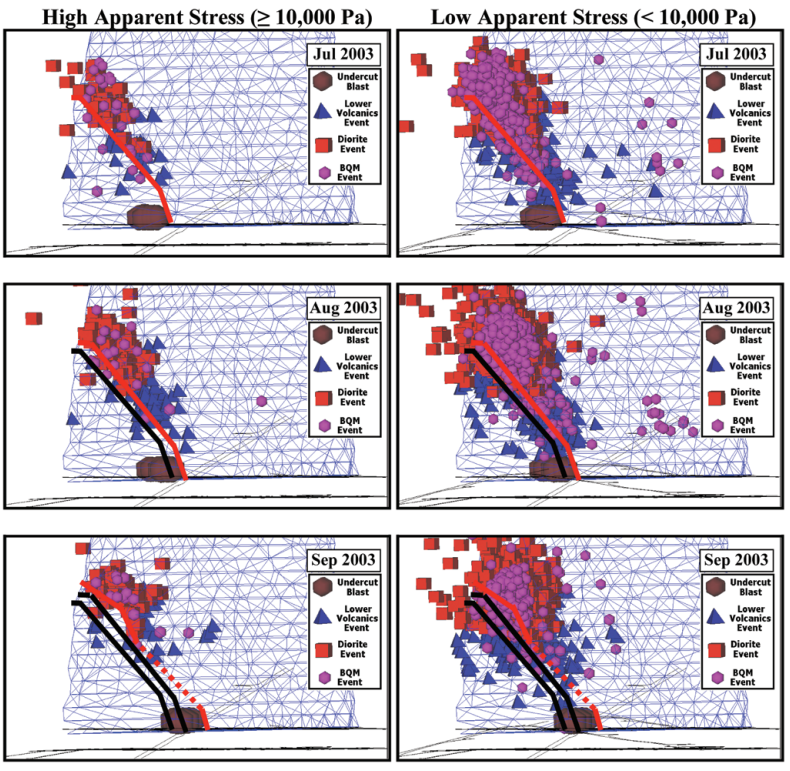

Figure 27—Month-by-month views looking north-west for July– Sept 2003. The diagrams on the left show events with apparent stress of 10 000 Pascals or more. The diagrams on the right show events with an apparent stress of less than 10 000 Pascals

and retained for reference). The figures also show the location of the of the lower Apparent Stress events (Apparent Stress < 10,000 Pascals).

It is observed that during undercutting, high Apparent Stress events occur in a peak or apex shape on the south-west side of the orebody. The band of high Apparent Stress events was tighter and generally moved in a more continuous manner with the undercutting, compared to lower Apparent Stress events. When the band of high Apparent Stress events moved (generally up and to the North-East), there were few or no high Apparent Stress events recorded below the band. This could be interpreted that the high Apparent Stress events identified the location of an active stress-related failure front. The lower Apparent Stress events were more dispersed than the high Apparent Stress events.

The lower Apparent Stress events occurred predominantly along the sides of a failure zone profile rather than in the peak of the apex. There were also numerous low Apparent Stress events to the west of the orebody, outside the cave profile. These lower Apparent Stress events were occurring in areas that would have had lower induced stresses than the apex of the cave.

There were comparatively few high apparent stress seismic events in the BQM unit. This is likely due to the BQM unit tending to not be in the peak of the cave, but may also be reflecting the higher strength of the BQM.

Cave back versus seismogenic zone location

A series of inclined open holes were drilled from the 9700 Level to monitor movement of the cave (approximately 230 metres above the undercut level). Dipping of the open holes was routinely undertaken to estimate the cave back location.

On August 03, 2003 measurements recorded the cave back at about 9470 to 9480 in hole D262 (located in the south-west corner of the cave). This is within 10 metres of the top of the undercut blasting. Figure 28 shows the location of the events in July 2003, with the bottom of the seismicity at about the 9540 Elevation. This suggests a rock mass loosening zone of 60 to 70 metres. Duplancic[7] found that the zone of loosening was approximately 15 metres in height during mining of Lift 1 at Northparkes.

Throughout the undercutting, the zone of loosening was typically 50 to 70 metres in thickness.

A stress driven undercutting failure model

An undercutting model for Lift 2 at Northparkes is proposed. For the first two months of undercutting (approximately 10% of the total undercut), a dome-shaped seismogenic zone forms and moves in a relatively consistent and expected manner. As undercutting continued, geological discontinuities begin to have a major role in the location of seismic events. Movements in the stress-failure front are relatively discontinuous and erratic, despite a near constant undercutting rate. The contact between the weaker volcanics and stronger BQM units became preferentially seismically active.

Early in the undercutting, movements in the seismogenic zone were directly triggered by mine blasts. Most seismic events occurred within a few hours of the undercut blasts. Later in the undercutting, rock mass failure was less directly related to individual blasts with high seismic event rates occurring for 1 to 3 days after blasts.

The rate of seismic events was surprisingly consistent for the first two phases of the undercutting (approximately 1/3 of the undercut). Once the undercut was fully extended to the north, the number of seismic events per blast increased significantly. This further supports the notion that rock mass failure in the first two stages of undercutting was induced directly by stress change related to undercut extraction. As the undercut widened to the east, in the third stage of undercutting, rock mass failure was increasingly driven by caving related rock mass failure mechanisms.

The seismogenic zone showed a poor correlation with the measured location of the cave back. There was an aseismic zone of loosening of up to 50 to 70 metres in height above the cave back. At Palabora, a zone of loosening of up to 60–80 metres was identified[25].

S:P energy ratio analysis suggests that shear of existing discontinuities was the most common seismic source mechanism. This was consistent throughout the undercutting period, and for all the major rock mass units.

The peak of the undercut seismogenic zone was the location of the highest apparent stress events. This suggests that the peak of the seismogenic zone represented an area of stress-driven rock mass failure.

There were significant areas above the undercut that had very few events. Different rock types had a different seismic response, the volcanics were far more seismically active than the quieter BQM in the east. Areas in which caving was not occurring under stress-driven failure were virtually aseismic. The east side of the cave had very few seismic events recorded. There were also very few seismic events in the northern 25% of the undercut area. These two anomalies are not adequately explained by a reduction in seismic system sensitivity, and may be more related to stress shadowing of undercut blasting by the caved muckpile and the loosened rock mass zones. It is unclear whether a significantly more sensitive seismic system would detect a significant number of events in the aseismic areas.

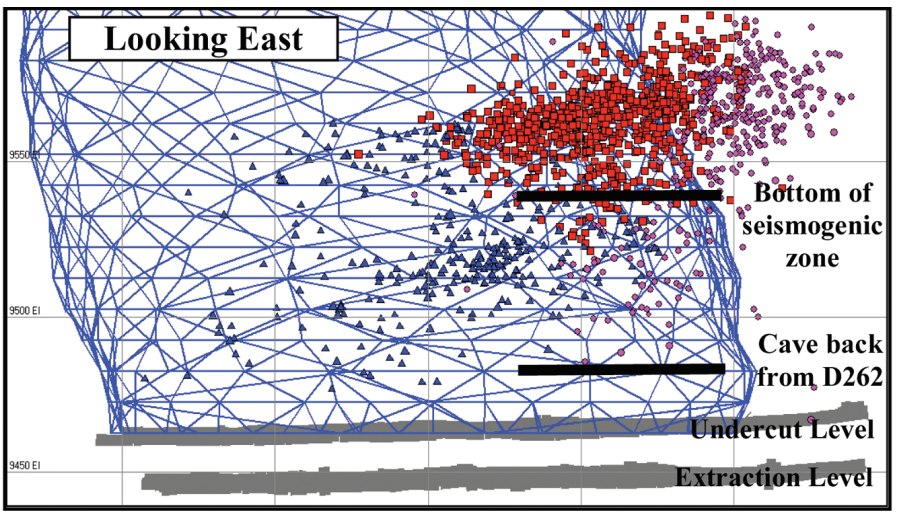

Figure 28—Seismic events for July 2003, which is the month prior to the open hole checking on August 03, 2003. The blue profile represents the final cave shape (as of Jan 2006). The bottom of the seismogenic zone in the south-west corner is at approximately 9530 to 9540 elevation. This is well above the cave back measured (using open holes) at 9470-9480 on 03 August 03 2003

Acknowledgements

Rio Tinto, in particular Northparkes, is gratefully acknowledged for permission to publish this paper. This work was conducted under contract to the Australian Centre for Geomechanics as part of the ACG research project 'Broadening the Application of Seismic Monitoring in Australian Underground Mines'. Financial sponsors of this project are: Agnico-Eagle Mines Limited, All-State Explorations, Barrick Gold of Australia, BHP Billiton—Nickel West, Corporación Nacional del Cobre de Chile, Harmony Gold Australia Ltd, Independence Group NL, Kalgoorlie Consolidated Gold Mines Pty Ltd, Kirkland Lake Gold Inc., Lionore Australia Pty Ltd, Minerals and Energy Research Institute of Western Australia, Newcrest Mining, Newmont Australia, Oxiana Limited, Perilya Mines N.L., Xstrata Copper, and Xstrata Zinc.

References

1. Duffield, S. Design of the second block cave at Northparkes E26 mine. *Proceedings MassMin 2000*, G. Chitombo (ed.), Australian Institute of Mining and Metallurgy: Melbourne, 2000, p. 334–346.
2. House, M., van As, A., and Dudley, J. Block Caving Lift 1 of the Northparkes E26 Mine, *Underground Mining Methods: Engineering Fundamentals and International Case Studies*, SME, Colorado, 2001. pp. 411–416.
3. Glazer, S.N., Lurka, A., Mutke, G., Dubinski, J., and Moss, A. Application of seismic tomography to block cave operations. Technical report to Rio Tinto.2005.
4. Chen, D. Geotechnical assessment of block cave mining in Northparkes Mines, NSW Australia, *Proc. 2nd North Am. Rock Mech. Symp.* M. Aubertin, F. Hassani and H.S.Mitri (eds.), Int. Soc. Rock Mech. 1996. p. 261.
5. Itasca. FLAC3D Modelling of the Lift 2 Undercut and Extraction-Level Development at Northparkes Mines, E26 Mine. Technical Report for Northparkes Mines. 2005.
6. Doolan, J. An analysis of microseismic activity at Northparkes mines during undercutting of the Lift 2 block cave project. Unpublished undergraduate thesis. RMIT. 2004. 77 pp.
7. Duplancic, P. Characterisation of caving mechanisms through analysis of stress and seismicity. Unpublished PhD thesis, Department of Civil and Resource Engineering, University of Western Australia. 2001. 227 pp.
8. Butcher, R. Caving Geomechanics. *Proceedings of ACG Seminar 0309*, 2003, Perth.
9. White, H., de Beer, W., van As, A., and Allison, D. Design and implementation of seismic monitoring systems in a block-cave environment. *Proceedings of Massmin 2004*, Santiago, Karzulowicz K. and Alfaro, M.A. (eds.) Chile, 2004. pp. 559–564.
10. Gutenberg, B. and Richter, C.F. Frequency of earthquakes in California, *Bulletin of the Seismological Society of America*, vol. 34, 1944, pp. 185–188.
11. Legge, N.B. and Spottiswoode, S.M. Fracturing and microseismicity ahead of a deep gold mine stope in the pre-remnant stages of mining. *Proceeding of the 6th Int. Congress on Rock Mech.*, Montreal, September 1987, 1987, pp. 1071–1078.
12. Gibowicz, S.J. and Kijko, A. *An introduction to mining seismology*. 1st edition San Diego: Academic Press. 1994.
13. Finnie, G.J. Some statistical aspects of mining induced seismic events. *Proceedings of SARES99, 2nd South African Rock Engineering Symposium*, Johannesburg, 13–15 September 1999. T.O. Hagan(ed.), Johannesburg, 1999. pp. 132–139.
14. Amidzic, D. Energy-moment relation and its application. *Proceedings of Rockbursts and Seismicity in Mines—RaSiM 5*, Johannesburg, September 2001. G. van Aswegen *et al.* (eds.), Johannesburg: South African Institute of Mining and Metallurgy, 2001. pp. 509–513.
15. Gibowicz, S.J., Young, R.P., Talebi, S., and Rawlence, D.J. Source parameters of seismic events at the underground research laboratory in Manitoba, Canada: scaling relations for events with moment magnitude smaller than –2. *Bull. Seismol. Soc. Am.* vol. 81, 1992. pp. 1157–1182.
16. Boatwright, J. and Fletcher, J.B. The partition of radiated energy between P and S waves. Bull. *Seismol. Soc. Am.* vol. 74, 1984. pp. 361–376.
17. Cichowicz, A., Green, R.W.E., Brink, A.v.Z, Grobler, P., and Mountfort, P.I. The space and time variation of micro-event parameters occurring in front of an active stope. *Proceedings of Rockbursts and Seismicity in Mines*. Minneapolis. C. Fairhurst (ed.). Rotterdam: A.A.Balkema, 1990, pp. 171–175.
18. Urbancic, T.I., Young, R.P., Bird, S., and Bawden, W. Microseismic source parameters and their use in characterizing rock mass behaviour: considerations from Strathcona mine. *Proceedings of 94th Annual General Meeting of the CIM: Rock Mechanics and Strata Control Sessions*, Montreal, 26–30 April 1992, 1992, pp. 36–47.
19. Sato, T. A note on body wave radiation from expanding tension crack. *Sci. Rep. Tohoku University*, Geophysics, 1978, pp. 1–10.
20. van Aswegen, G. and Butler, A.G. Applications of quantitative seismology in South African gold mines. *Proceedings 3rd International Symposium on Rockburst and Seismicity in Mines*. R.P. Young (ed.). Kingston, A.A. Balkema, 1993, pp. 261–266.
21. Simser, B.P., Falmagne, V., Gaudreau, D., and MacDonald, T. Seismic Response to Mining at the Brunswick Mine. CIM Annual General Meeting. Montreal. 2003. 12 pp.
22. Mendecki, A.J., van Aswegen, G., and Mountfort, P. A guide to routine seismic monitoring in mines. Chapter 9. *A Handbook on Rock Engineering Practice for Tabular Hard Rock Mines*. A.J. Jager and J.A. Ryder (eds.), Creda Communications, Cape Town, 1999.
23. Mendecki, A.J. and van Aswegen, G. Seismic monitoring in mines: selected terms and definitions. *Proceedings of Rockbursts and Seismicity in Mines —RaSiM 5*, Johannesburg, September 2001. G. van Aswegen, R. Durrheim, and W.D.Ortlepp (eds.), South African Institute of Mining and Metallurgy, 2001, Johannesburg. pp 563–570.
24. Wyss, M. and Brune, J.N. Seismic moment, stress and source dimensions for earthquakes in the California-Nevada region. *Journal of Geophysical Research*, vol. 73, 1968, pp. 4681–4694.
25. Glazer, S.N. and Hepworth, N. Crown pillar failure mechanism—case study based on seismic data from Palabora Mine. *IMM Transactions—Mining Technology*. vol. 115. no. 2. 2006. pp. 75–84.
26. Chen, D. Application of a microseismic system in monitoring at E26 block cave at Northparkes Mines, Australia, *Proc. Int. Conf. on Geomech*. N.I. Aziz and B. Indraranta (eds.), 2, Wollongong, Australia., 1998, pp. 1067–1078.
27. Hudyma, M.R. Self-similar clustering of seismic events in mines. PhD in progress, University of Western Australia, 2007. ◆